



**HAL**  
open science

# The ammonites of the Les Ferres Aptian Basin (Lower Cretaceous, Southeast of France): the genus *Toxoceratoides* (Ancyloceratina, Helicancyllidae)

Stéphane Bersac, Didier Bert

► **To cite this version:**

Stéphane Bersac, Didier Bert. The ammonites of the Les Ferres Aptian Basin (Lower Cretaceous, Southeast of France): the genus *Toxoceratoides* (Ancyloceratina, Helicancyllidae). *Cretaceous Research*, 2021, 118, pp.104661. 10.1016/j.cretres.2020.104661 . insu-02966450

**HAL Id: insu-02966450**

**<https://insu.hal.science/insu-02966450>**

Submitted on 14 Oct 2020

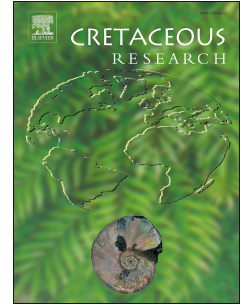
**HAL** is a multi-disciplinary open access archive for the deposit and dissemination of scientific research documents, whether they are published or not. The documents may come from teaching and research institutions in France or abroad, or from public or private research centers.

L'archive ouverte pluridisciplinaire **HAL**, est destinée au dépôt et à la diffusion de documents scientifiques de niveau recherche, publiés ou non, émanant des établissements d'enseignement et de recherche français ou étrangers, des laboratoires publics ou privés.

# Journal Pre-proof

The ammonites of the Les Ferres Aptian Basin (Lower Cretaceous, Southeast of France): the genus *Toxoceratoides* (Ancyloceratina, Helicancyllidae)

Stéphane Bersac, Didier Bert



PII: S0195-6671(20)30347-5

DOI: <https://doi.org/10.1016/j.cretres.2020.104661>

Reference: YCRES 104661

To appear in: *Cretaceous Research*

Received Date: 13 May 2020

Revised Date: 11 August 2020

Accepted Date: 26 September 2020

Please cite this article as: Bersac, S., Bert, D., The ammonites of the Les Ferres Aptian Basin (Lower Cretaceous, Southeast of France): the genus *Toxoceratoides* (Ancyloceratina, Helicancyllidae), *Cretaceous Research*, <https://doi.org/10.1016/j.cretres.2020.104661>.

This is a PDF file of an article that has undergone enhancements after acceptance, such as the addition of a cover page and metadata, and formatting for readability, but it is not yet the definitive version of record. This version will undergo additional copyediting, typesetting and review before it is published in its final form, but we are providing this version to give early visibility of the article. Please note that, during the production process, errors may be discovered which could affect the content, and all legal disclaimers that apply to the journal pertain.

© 2020 Elsevier Ltd. All rights reserved.

1       **The ammonites of the Les Ferres Aptian Basin (Lower Cretaceous,**  
2       **Southeast of France): the genus *Toxoceratoides* (Ancyloceratina,**  
3       **Helicancyllidae)**

4  
5                               Stéphane Bersac <sup>a, \*</sup> and Didier Bert <sup>a, b, c</sup>

6  
7   <sup>a</sup> Laboratoire du Groupe de recherche en paléobiologie et biostratigraphie des  
8   Ammonites (GPA), Bois-Mésanges, quartier Saint-Joseph, F-04170 La Mure-  
9   Argens, France

10   <sup>b</sup> Réserve naturelle nationale géologique de Haute-Provence, service  
11   Environnement, Conseil départemental des Alpes de Haute-Provence, 13, rue du  
12   Docteur-Romieu, CS 70216, F-04995 Digne-Les-Bains cedex 9, France

13   <sup>c</sup> Laboratoire Géosciences, UMR-CNRS 6118, université de Rennes-1, campus  
14   Beaulieu, bâtiment 15, F-35042 Rennes cedex, France

15   \* Corresponding author: geosteber@yahoo.fr (S. Bersac)

16  
17   Abstract:

18 *Toxoceratoides* (Ancyloceratina, Helicancyllidae) is a lower Aptian (Lower  
19 Cretaceous) small heteromorph ammonoid mainly known by small samples of  
20 fragmentary specimens. In the present work, we study a sample of 145  
21 specimens of this genus from the *Deshayesites forbesi*, *Deshayesites deshayesi*  
22 and *Dufrenoyia furcata* zones (lower Aptian) of the vicinity of the village of Les  
23 Ferres (southeastern France). The taxa recognized (in stratigraphic order) are:  
24 *Toxoceratoides* sp., *Toxoceratoides royerianus* (d'Orbigny, 1842) and  
25 *Toxoceratoides rochi* Casey, 1961. Their ontogenetic sequence is described; the  
26 intraspecific variability of *Toxoceratoides rochi* is considerable and it concerns  
27 adult size, coiling, duration of the ontogenetic stages and ornamentation. No  
28 sexual dimorphism is recognized. The main evolutionary pattern of the genus  
29 consists in the replacement of primitive ribs (here named 'royerianus ribs') by  
30 derived ribs ('rochi ribs') on the flexus and retroversum. The genus  
31 *Toxoceratoides* could be used as a biostratigraphic tool.

32

33 Key words: heteromorph ammonite; evolution; ontogeny; intraspecific  
34 variability; heterochronic variation.

35

36 1. Introduction

37

38 The Les Ferres Aptian Basin (LFAB) is a small subsident basin nowadays  
39 located in the vicinity of the village of Les Ferres, in the Estéron valley (Alpes-  
40 Maritimes department, southeastern France, Bersac and Bert, 2019, Fig. 1). The  
41 location of the outcrops studied and the lower Aptian litho- and biostratigraphy  
42 of the LFAB have been previously described in Bersac and Bert (2019). The  
43 LFAB is characterized by relatively thick lower Aptian deposits particularly rich  
44 in macrofossils, especially ammonites (fossil cephalopods, Bersac and Bert,  
45 2019). The age of these series extends from the *Deshayesites forbesi* Zone (in  
46 the sense of Bersac et al., 2012) to the late *Dufrenoyia furcata* Zone (*Dufrenoyia*  
47 *dufrenoyi* Subzone, Fig. 2). Its ammonite fauna is remarkable by the significant  
48 proportion of heteromorphs of the families Ancyloceratidae Meek, 1876 and  
49 Helicancyllidae Hyatt, 1894 (=Acrioceratidae Vermeulen, 2004). In the LFAB,  
50 the lower Aptian Helicancyllidae are only represented by the genus  
51 *Toxoceratoides* Spath, 1924 (Bersac and Bert, 2019), which is a small tripartite  
52 shelled heteromorph genus (the shell of *Toxoceratoides* is composed of a  
53 proversum, a flexus and a retroversum, Casey, 1961a; Aguirre-Urreta, 1986;  
54 Avram, 2002; Bulot et al., 2018, Fig. 3). The aim of the present work is to  
55 describe and figure the *Toxoceratoides* of the LFAB, based on a sample of 145  
56 specimens from the *D. forbesi*-*D. furcata* zones interval.

57

## 58 2. Material and method

59

## 60 2.1. Material

61

62 The litho- and biostratigraphic framework based on ammonites of the LFAB and  
63 the sections from which the studied material originates are detailed in Bersac  
64 and Bert (2019).

65 The material studied is composed of 145 specimens of *Toxoceratoides* from 6  
66 sections of the LFAB. The specimens originate from: (1) the top of the  
67 Hauterivian-Aptian limestones (*Deshayesites forbesi* Zone, 1 specimen), (2) the  
68 *Ammonitoceras* Level of the Pont de la Cerise Member (*Deshayesites*  
69 *multicostatus* Subzone of the *Deshayesites deshayesi* Zone, 1 specimen) and (3)  
70 from the Les Graous Member (*Deshayesites grandis* Subzone of the *D.*  
71 *deshayesi* Zone and *D. furcata* Zone, 143 specimens). They are represented by  
72 marly-calcareous internal moulds, mostly deformed and fragmentary. The  
73 studied material is curated by the Réserve naturelle nationale géologique de  
74 Haute-Provence (RNNGHP, Digne-les-bains, France). The list of the studied  
75 specimens is given in Supplementary Appendix.

76

## 77 2.2. Method

78

79 The terminology used for describing the studied specimens and the criteria for  
80 determining them are based on the works of Frau et al. (2017) and Bulot et al.  
81 (2018). The variable H is the whorl height at the middle of the flexus (Fig. 3).

82 The ontogenetic sequence of the genus *Toxoceratoides* shows 3 successive  
83 stages (Fig. 3):

84 - Stage *i* (Bulot et al., 2018, p. 189) is adorned with uniform, simple and  
85 atuberculate ribs or ribs bearing a single ventrolateral tubercle.

86 - Stage *ii* presents an '*alternation of (...) primary ribs and atuberculate*  
87 *intercalatories*' (Bulot et al., 2018, p. 189). The main ribs are tuberculate and  
88 attenuated on the siphonal area. They are usually separated by one or more  
89 atuberculate intercalary ribs but can be more rarely contiguous. The intercalary  
90 ribs are generally not attenuated on the siphonal area. Stage *ii* can be subdivided  
91 in an early part named here '*stage iia*' with bituberculate main ribs (lateral and  
92 lateroventral tubercles, see Bulot et al., 2018, fig. 2R) and a late part named here  
93 '*stage iib*' with trituberculate main ribs (laterodorsal, lateral and lateroventral  
94 tubercles).

95 - Stage *iii* (Bulot et al., 2018, p. 189) is represented by various types of ribs: (1)  
96 simple and atuberculate ribs named here ‘rochi ribs’ because they predominate  
97 in the species *Toxoceratoides rochi* Casey, 1961 (Frau et al., 2017; Bulot et al.,  
98 2018); (2) bifid ribs with a laterodorsal tubercle named here ‘royerianus ribs’  
99 because they predominate in the species *Toxoceratoides royerianus* (d’Orbigny,  
100 1842) (Bulot et al., 2018); and (3) ribs with intermediate pattern (single with a  
101 laterodorsal tubercle or atuberculate and bifid).

102 According to Bulot et al. (2018), the species *Toxoceratoides royerianus* evolves  
103 toward the species *Toxoceratoides rochi* by the replacement of ontogenetic stage  
104 *iii*’s royerianus ribs by rochi ribs and by the change in shape of stage *ii*’s  
105 lateroventral tubercles. Thus, we consider the proportion of rochi ribs relative to  
106 the total number of ribs of stage *iii* as a diagnostic character. We calculated such  
107 proportion for the samples of each lithostratigraphic unit of the LFAB when  
108 possible. We studied the distributions of H and of the proportion of rochi ribs  
109 through frequency histograms and a Shapiro-Wilk normality test (Hammer and  
110 Harper, 2006) for the only significantly larger subzonal sample (over 30  
111 specimens), namely the sample from the *D. furcata* Subzone. They were  
112 performed using the software PAST version 2.17c (Hammer et al., 2001,  
113 <http://folk.uio.no/ohammer/past/>).



114 Our taxonomic approach is based on a ‘palaeobiologic’ concept of the species  
115 rather than a typologic concept (see discussions about these concepts in Bert,  
116 2013; De Baets et al., 2015).

117 The database of the studied specimens is available in Supplementary Appendix.

118

### 119 3. Results

120

#### 121 3.1. Descriptive paleontology

122

123 Order Ammonoidea Zittel, 1884

124 Suborder Ancyloceratina Wiedmann, 1966

125 Superfamily Ancyloceratoidea Gill, 1871

126 Family Helicancyllidae Hyatt, 1894

127

128 *Taxonomic considerations about the family-group name Helicancyllidae.* The  
129 opinions of recent authors differ on the suprageneric classification of  
130 *Toxoceratoides*: it could belong to the family Helicancyllidae (Bert, 2009), to the  
131 family Acrioceratidae (Vermeulen, 2004; Bulot in Vincent et al., 2010; Frau et

132 al., 2017) or to the subfamily Helicancylinae of the family Ancyloceratidae (see  
133 Casey, 1961a; Aguirre-Urreta, 1986; Kakabadze and Hoedemaeker, 2004;  
134 Kakabadze in Klein et al., 2007, footnote p. 94). Here, we consider that the  
135 genus *Toxoceratoides* belongs to a family distinct from the Ancyloceratidae on  
136 the basis of the phylogenetic arguments developed by Bert (2009), and we use  
137 the family-group name Helicancyllidae for the following reasons:

138 - (1) following Bert (2009) and Bulot (in Vincent et al., 2010), we consider that  
139 the family-groups Helicancyllidae and Acrioceratidae share the same taxonomic  
140 content and that both the two names designate the same family;

141 - (2) the family-group names Helicancyllidae and Acrioceratidae meet all the  
142 requirements of availability outlined in Articles 11 and 12 of the International  
143 Code of Zoological Nomenclature (ICZN). Both are thus available in the sense  
144 of the ICZN (see also Article 10.6);

145 - (3) according to the Principle of Priority (ICZN, Article 23), the name  
146 Helicancyllidae, Hyatt, 1894 has seniority on the name Acrioceratidae,  
147 Vermeulen, 2004.

148

149 *Toxoceratoides* sp.

150 Fig. 4A

151

152 2019 *Toxoceratoides* sp. - Bersac and Bert, p. 155, fig. 12.

153

154 *Material* (see *Supplementary Appendix*). 1 specimen from the top of the  
155 Hauterivian-Aptian limestones (Bed 400 of CLE section, *Deshayesites forbesi*  
156 Zone).

157

158 *Description*. The specimen is a fragment of flexus and retroversum with H = 9  
159 mm. Only one side of the specimen is preserved and its width cannot thus be  
160 measured. Its ventral area is not preserved. The ornamentation is only composed  
161 of royerianus ribs (slightly rursiradiate, thin, relatively dense and arising in pairs  
162 from a laterodorsal tubercle). Apart the laterodorsal tubercle, these ribs do not  
163 bear additional tubercle. The septal suture is not observable. The proportion of  
164 rochi ribs is 0% (Table 1).

165

166 *Discussion*. This specimen is quoted in Bersac and Bert (2019, p. 157, fig. 12). It  
167 originates from a bed (Bed 400 of CLE section) assigned to the lower part of the  
168 *D. forbesi* Zone. Its ornamentation corresponds to the ontogenetic stage *iii*. The  
169 specimen shows primitive characteristics with a proportion of rochi ribs of 0%

170 (ornamentation of its stage *iii* only represented by royerianus ribs). This  
171 specimen may correspond to a primitive form of *Toxoceratoides*, just like those  
172 figured by Avram (2002, pl. 1, figs. 9a, b, 12a-c, pl. 2, figs. 9, 12) and Delanoy  
173 et al. (2008, pl. 11, fig. 4a, b). Our specimen differs from the lower Aptian small  
174 heteromorph genus *Volgoceratoides* Mikhailova and Baraboshkin, 2002  
175 (Mikhailova and Baraboshkin, 2002, p. 544) by its less distant ribs and its lower  
176 position of the rib furcation point on the flexus and proversum. The imprecise  
177 biostratigraphic position and the very fragmentary state of preservation of the  
178 studied specimen prevent us to identify it at species level.

179

180 *Biostratigraphic distribution.* *Deshayesites forbesi* Zone of the LFAB.

181

182 *Toxoceratoides royerianus* (d'Orbigny, 1842)

183 Fig. 4B-G

184

185 2019 *Toxoceratoides* aff. *royerianus* - Bersac and Bert, p. 155, 163, 164, figs. 5,  
186 7, 10, 12, pl. 3, figs. 13-16.

187 For an extensive synonymy of this species, see Bulot et al. (2018).

188

189 *Material (see Supplementary Appendix)*. 1 specimen from Bed 405 of VAL  
190 section (*D. multicosatus* Subzone, *D. deshayesi* Zone) and 10 specimens from  
191 the *Toxoceratoides* Bed (*D. grandis* Subzone, *D. deshayesi* Zone) of GRS1,  
192 CLE and CHP sections. These 11 specimens were identified as *Toxoceratoides*  
193 aff. *royerianus* in Bersac and Bert (2019).

194

195 *Description of the material of the D. multicosatus Subzone (D. deshayesi Zone)*.  
196 The specimen No. SBC.06061-00003/VAL066 (Fig. 4B) is the only  
197 Helicancyliidae we collected in the *D. multicosatus* Subzone (*D. deshayesi*  
198 Zone) of the LFAB. It was identified as *Toxoceratoides* aff. *royerianus* in  
199 Bersac and Bert (2019, fig. 7). This specimen is a fragment of flexus and  
200 retroversum with H=13.9 mm. Only one side of the specimen is preserved. The  
201 ornamentation of the flexus is represented by thick and straight main ribs  
202 bearing lateroventral and smaller lateral tubercles. The shape of the lateroventral  
203 tubercles is conical, slightly sagittally compressed. It is not possible to  
204 determine if these ribs bear or not a laterodorsal tubercle since the  
205 ornamentation is poorly preserved on the dorsal margin of the flexus. These  
206 main ribs are separated by one straight, thin and atuberculate intercalary rib.  
207 This ornamentation corresponds to the stage *ii*. On the retroversum, stage *ii* is

208 replaced by stage *iii*. Its ribs are simple and atuberculate (rochi ribs) or arise in  
209 pairs from a laterodorsal tubercle (royerianus ribs). The peristome is not  
210 preserved and the septal suture is not observable. The proportion of rochi ribs is  
211 42.85% for this specimen (Table 1).

212

213 *Description of the material of the D. grandis Subzone (D. deshayesi Zone)*. The  
214 10 specimens of the *D. grandis* Subzone (*D. deshayesi* Zone) are all fragments  
215 but it is nevertheless possible to follow their ontogeny from a specimen to  
216 another. H has been measured only on 5 specimens; it varies from 7.2 mm to  
217 11.7 mm with a mean value of 10.04 mm (Table 1).

218 The ornamentation is visible from a whorl height of 1 mm and corresponds to  
219 the stage *ii*a (Fig. 4F). It is represented by simple, uniform, straight and  
220 rectiradiate ribs attenuated on the siphonal area. These ribs bear a lateroventral  
221 and a smaller lateral tubercle.

222 From a whorl height of 2.7 mm (Fig. 4F), ornamentation changes and  
223 corresponds to stage *ii*b: the ribs become slightly prorsiradiate and the siphonal  
224 area becomes smooth to subsmooth. The main ribs bear a laterodorsal, a lateral  
225 and a larger lateroventral tubercle. This latter can be conical or claviform. Two  
226 main ribs are separated from each other by a single thin and atuberculate  
227 intercalary rib (Figs 4F, G).

228 At the beginning of the flexus, stage *iib* is abruptly replaced by stage *iii* (Bersac  
229 and Bert, 2019, pl. 3, figs. 13, 14). Its ornamentation is represented by slightly  
230 rursiradiate ribs that can be of royerianus, rochi or intermediate type. Most of  
231 the specimens exhibit a mixture of each type of ribs (Fig. 4C1-D2, Bersac and  
232 Bert, 2019, pl. 3, figs. 15, 16). One specimen (SBC.06061-00006/CHP038, Fig.  
233 4E1, E2) exhibits some ribs bearing a discrete lateroventral tubercle. The  
234 royerianus ribs seem to predominate on the flexus and the beginning of the  
235 retroversum whereas the rochi ribs seem to be more frequent on the distal part of  
236 the retroversum (Fig. 4C1, C2). On the proversum, the flexus and the  
237 retroversum, the dorsal area is adorned with dense and thin ribs concave towards  
238 the peristome. No specimen has its peristome preserved. The septal suture is not  
239 observable. The proportion of rochi ribs has been measured on 4 specimens: it  
240 ranges from 30% to 61.53% and is 47.88% on average (Table 1).

241

242 *Remarks on the biostratigraphic position of T. royerianus in its type-stratum.* *T.*  
243 *royerianus* was recently revised by Bulot et al. (2018) on the basis of topotype  
244 material from the *Argiles à Plicatules* (a lower Aptian formation of the Paris  
245 Basin, see Corroy, 1925; Amédéo and Matrimon, 2004; Bersac and Bert, 2015,  
246 2018, 2020). Bulot et al (2018, fig. 3) argued that this formation ranges from the  
247 *D. forbesi* Zone to the *Epicheloniceras martini* Zone and that *T. royerianus*

248 cannot thus be precisely dated. We do not agree on this point. We studied the  
249 material figured by Bulot et al. (2018, excepting the specimen figured fig. 3(3))  
250 and numerous additional representatives of *T. royerianus* from the *Argiles à*  
251 *Plicatules* deposited in various French public institutions (a list of these  
252 institutions is given in Bersac and Bert, 2015, p. 270).

253 Actually, the taphonomic characteristics of the whole *Toxoceratoides* of the  
254 *Argiles à Plicatules* we could study are the same as those of the sample of the *D.*  
255 *deshayesi* Subzone's small pyrite ammonites (*D. deshayesi* Zone, Bersac and  
256 Bert, 2015, 2018). The *Toxoceratoides* are thus part of this taphopopulation and  
257 are assigned to the *D. deshayesi* Subzone too. Moreover, we consider that the  
258 syntype of *Megatyloceras ricordeanum* (d'Orbigny, 1850) and the lectotype of  
259 *Deshayesites deshayesi* (d'Orbigny, 1841) (respectively figured in Bulot et al.,  
260 2018, figs. 3(1) and 3(2)) are contemporaneous and assigned to the *D. deshayesi*  
261 Subzone too (see Bersac and Bert, 2015, 2018 for explanations).

262 Concerning the taxonomic identification of the specimens figured by Bulot et al.  
263 (2018), we disagree about the following determinations proposed by these  
264 authors:

265 - The specimen figured under *Dufrenoyia* sp. in Bulot et al. (2018, fig. 3(4)) is in  
266 our opinion a *Deshayesites* whose characters fall into the range of variability of  
267 *D. deshayesi* (see Bersac and Bert, 2015).



268 - The specimen figured under *Epicheloniceras* sp. (Bulot et al., 2018, fig. 3(6))  
269 bears neither the trituberculate ribs nor the ventral depression typical of this  
270 genus. We interpret it as a robust representative of *Cheloniceras cornuelianum*  
271 (d'Orbigny, 1842) (see Bersac and Bert, 2018); its taphonomic characteristics  
272 are those of the *D. deshayesi* Subzone's small pyritic ammonites of the *Argiles à*  
273 *Plicatules*.

274 - The specimen figured under *Dufrenoyia* gr. *dufrenoyi* (Bulot et al., 2018, fig.  
275 3(5)) is indeed a representative of the genus *Dufrenoyia* Kilian and Reboul,  
276 1915, but its black matrix clearly differs from that of the specimens of the *D.*  
277 *deshayesi* Subzone of the *Argiles à Plicatules*. This indicates that this specimen  
278 does not belong to the *D. deshayesi* Subzone of this formation but comes from a  
279 different level (for a discussion on the presence of the genus *Dufrenoyia* in the  
280 *Argiles à Plicatules* see Bersac and Bert, 2018). It is to note that this *Dufrenoyia*  
281 belongs to the famous Swiss paleontologist François-Jules Pictet de la Rive's  
282 (1809-1872) collection (Lionel Cavin, personal communication) and not to the  
283 Antoine Pictet's collection ('A. Pictet' coll. in Bulot et al., 2018, caption of fig.  
284 3(5)).

285 In our opinion, the specimens figured by Bulot et al. (2018, figs. 2, 3) do not  
286 contradict the fact that the topotype material of *T. royerianus* is assigned to the  
287 *D. deshayesi* Subzone (*D. deshayesi* Zone). This age is consistent with the

288 observations Bulot et al. (2018, p. 193) made in southern France, where ‘T.  
289 royeri occurs in the upper part of the *D. forbesi* Zone’ (the Bersac et al.’s (2012)  
290 *D. deshayesi* Subzone corresponds to the upper part of the Reboulet et al.’s  
291 (2014, 2018) *D. forbesi* Zone, Fig. 2).

292

293 *Evolutionary characters of the Toxoceratoides of the D. deshayesi Zone in the*  
294 *literature.* Some specimens figured in the literature and assigned to the *D.*  
295 *deshayesi* Zone have their flexus and retroversum preserved, which allows  
296 comparisons with the material of the LFAB:

297 - One specimen from the *Cheloniceras parinodum* Subzone (= *D. multicosatus*  
298 Subzone in Bersac et al., 2012) of southern England was figured under *T.*  
299 *royerianus* by Casey (1960, pl. VI, figs. 2a, 2b). Its retroversum seems to exhibit  
300 a mixture of royerianus and rochi ribs. Following Bulot et al. (2018, p. 190), we  
301 consider this specimen as a *T. royerianus*.

302 - The specimen figured under *T. aff. royerianus* by Conte (1999, fig. 6)  
303 originates from Serviers-et-Labaume (southern France) lower Aptian’s Bed 2  
304 (‘*Serviers-la-Baume*’, ‘niveau 2’ in Conte, 1999, p. 11, fig. 1). This bed seems  
305 to be assigned to the *D. grandis* Subzone because it has provided *Deshayesites*  
306 Kasansky, 1914 identified as *Deshayesites grandis* var. *lacertosus* Casey, 1964  
307 and *Deshayesites vectensis* Spath, 1930 by Conte (1999, p. 11). The specimen of

308 *Toxoceratoides* from Bed 2 bears a majority of royerianus ribs, thus we consider  
309 it as a representative of *T. royerianus*.

310 - The specimens identified under *Toxoceratoides subproteus* Casey, 1961 by  
311 Casey (1980, p. 651, pl. CIII, fig. 3) and under *Tonohamites decurrens* Spath,  
312 1924 by the same author (1960, pl. V, fig. 3; 1961a, pl. XXI, fig. 2B) originate  
313 from Scaphites Beds' Bed 15 ('bed 3' in Casey, 1961b, p. 510) of Atherfield  
314 Bay (Isle of Wight, southern England, see Casey et al., 1998, p. 517-519), which  
315 is the last bed of the *D. grandis* Subzone in this section. Following Bulot et al.  
316 (2018), we consider these specimens as representatives of the genus  
317 *Toxoceratoides* and not *Tonohamites* Spath, 1924. Contrary to the specimens of  
318 the *D. grandis* Subzone of the LFAB, these English specimens bear a majority  
319 of rochi ribs on their stage *iii* and we thus assign them to *T. rochi*. Consequently,  
320 the *Toxoceratoides* of the *D. grandis* Subzone of the LFAB (Vocontian Basin)  
321 bear more primitive characters (significant proportion of royerianus ribs and  
322 thus low proportion of rochi ribs) than the *Toxoceratoides* of the upper *D.*  
323 *grandis* Subzone of Atherfield (Anglo-Paris Basin) that bear a significant  
324 proportion of rochi ribs. If one supposes that the evolution of the proportion of  
325 rochi ribs is synchronous between the Vocontian Basin and the Anglo-Paris  
326 Basin, the *Toxoceratoides* of the LFAB's *Toxoceratoides* Bed are slightly earlier  
327 within the *D. grandis* Subzone than the *Toxoceratoides* of Scaphites Beds' Bed  
328 15 of Atherfield. These elements suggest that *T. royerianus* occurs at least from

329 the *D. deshayesi* Subzone to the *D. grandis* Subzone (*D. deshayesi* Zone) and  
330 that the transition between *T. royerianus* and *T. rochi* may occur within the *D.*  
331 *grandis* Subzone.

332 - The specimen identified as *Toxoceratoides royerianus* from the *Audouliceras*  
333 *renauxianum* Subzone (upper *D. deshayesi* Zone) of the Middle Volga area  
334 (Central Russia) by Baraboshkin and Mikhailova (2002, pl. VI, fig. 6) presents  
335 an irregular alternation of main trituberculate and atuberculate ribs on its  
336 proversum and a flexus and retroversum bearing a mixture of possible rochi and  
337 intermediate or royerianus ribs. This specimen is remarkable by the presence of  
338 a spire with whorls in contact (this latter character seems to be uncommon in  
339 *Toxoceratoides*, see Aguirre-Urreta, 1986; Avram, 2002; Frau et al., 2017; Bulot  
340 et al., 2018). As far as we know, no other Helicancyliidae from the *A.*  
341 *renauxianum* Subzone of the Middle Volga area has been figured or described.  
342 In our opinion, additional data on the lower Aptian Helicancyliidae from this  
343 area are required to identify this specimen to the species level.

344

345 *Discussion on the identification of the Toxoceratoides from the D. multicosatus*  
346 *and D. Grandis subzones of the LFAB.* Following Frau et al. (2017) and Bulot et  
347 al. (2018), the main diagnostic characters of *T. royerianus* (*'T. royeri'* in Bulot  
348 et al., 2018) are (1) the predominance of stage *iii*'s royerianus ribs whereas rochi

349 ribs predominate in its daughter species *T. rochi* and (2) the lateroventral  
350 tubercles of stage *ii* that are less prominent and less flattened in *T. royerianus*  
351 than in *T. rochi*.

352 The *Toxoceratoides* of the *D. grandis* Subzone of the LFAB have a stage *iii*  
353 characterized by a mixture of royerianus and rochi ribs, with a significant  
354 proportion of royerianus ribs. We thus assigned them to *T. royerianus*.

355 The only specimen of *Toxoceratoides* from the *D. multicostatus* Subzone of the  
356 LFAB has a stage *iii* characterized by a mixture of royerianus and rochi ribs too.  
357 Because (1) this specimen exhibits evolutionary characters of *T. royerianus*,  
358 because (2) it is temporally located between two populations of *Toxoceratoides*  
359 with the same evolutionary characters (earlier topotype *T. royerianus* from the  
360 *D. deshayesi* Subzone of the Paris Basin and later *T. royerianus* of the *D.*  
361 *grandis* Subzone of the LFAB) and because (3) these two latter populations are  
362 both identified as *T. royerianus*, we identified this specimen as *T. royerianus*  
363 too, despite its fragmentary state of preservation.

364 *Biostratigraphic distribution.* *Deshayesites deshayesi*, *Deshayesites*  
365 *multicostatus* and *Deshayesites grandis* subzones (*Deshayesites deshayesi*  
366 Zone).

367

368 *Toxoceratoides rochi* Casey, 1961

369 Figs. 4H-P4, 5, 7

370

371 2011 *Tonohamites* sp. - Bert and Bersac, fig. 42

372 2019 *Toxoceratoides rochi* - Bersac and Bert, p. 155, 165, figs. 5, 9, 10, 12, 15,

373 pl. 5, figs. 1-4

374 For an extensive synonymy of this species, see Frau et al. (2017).

375

376 *Material* (see *Supplementary Appendix*). 130 specimens from the *D. furcata*

377 Subzone and 3 specimens from the *D. dufrenoyi* Subzone (*D. furcata* Zone)

378 from GRS1, CHP and GRO sections.

379

380 *Description of the sample of the D. furcata Subzone*. Most of the 130 specimens

381 of this sample are fragmentary but they allow a good overview of the

382 ontogenetic sequence. The sample is characterized by a very important

383 morphological disparity.

384 The two subcomplete specimens of the sample are 82.7 mm (SBC.06061-

385 00001/GRS398, Fig. 4P1-P4) and 73.8 mm (SBC.06061-00001/GRS383, Fig.

386 5J) in total length. H was measured for 60 specimens, including 57 specimens  
387 from GRS1 section (Supplementary Appendix). Most of the specimens are  
388 deformed, which implies that the value of H has to be considered as an  
389 estimation. This values varies by a factor of two (from 8 to 16.7 mm) with an  
390 average around 13 mm. According to the fitted normal curve of its histogram,  
391 the distribution of H seems bimodal (Fig. 6) but it does not significantly depart  
392 from normality ( $p=0.512$ ). Specimens with small whorl height are exemplified  
393 by SBC.06061-00001/GRS206 (Fig. 5A1, A2) and SBC.06061-00001/GRS366  
394 (Fig. 5G); intermediate specimens are illustrated by SBC.06061-00001/GRS287  
395 (Fig. 4L) and SBC.06061-00001/GRS591 (Fig. 5I); larger ones are represented  
396 by SBC.06061-00001/GRS198 (Fig. 5Q1, Q2) and SBC.06061-00001/GRS527  
397 (Fig. 5D).

398 The shell is planispiraled (no helical specimen was observed). The earliest  
399 developments of the proversum are observable from a whorl height of 0.8 mm  
400 (Fig. 7I, J, L) and they never exhibit any spiral. The proversum is more or less  
401 curved. The angle between the proversum and retroversum is variable from a  
402 specimen to another: SBC.06061-00001/GRS580 (Fig. 5O1) and SBC.06061-  
403 00001/GRS221 (Fig. 5H1) have a rather narrow angle, whereas SBC.06061-  
404 00001/GRS284 (Fig. 4H) and SBC.06061-00001/GRS383 (Fig. 5J) have an  
405 open angle. The retroversum seems to reach a significant length in some  
406 specimens (Fig. 7G).

407 The ornamentation and duration of the ontogenetic stages vary significantly  
408 from a specimen to another:

409 - Stage *i* is composed of dense and thin ribs that can be atuberculate or bear a  
410 discrete lateroventral tubercle. These ribs do not attenuate when crossing the  
411 siphonal area. This stage is generally present in the earliest part of the  
412 proversum (Fig. 7I, L), but its duration strongly varies from a specimen to  
413 another: it can be very short (Fig. 4J1-J4), intermediate (Fig. 4P1-P4, Fig. 5C)  
414 or more rarely can be present on nearly the entire proversum. In this last case,  
415 the specimens have a very slender shape (Fig. 7G, H).

416 - Stage *ii* is represented by tuberculate main ribs and atuberculate intercalary  
417 ribs. The ribs are generally simple, straight, rectiradiate or prorsiradiate and  
418 attenuated on the siphonal area (Fig. 4M). The main ribs first bear a lateral and a  
419 lateroventral tubercle (stage *ii**a*). They are rarely separated by one or more  
420 atuberculate intercalary ribs. Thereafter, a laterodorsal tubercle arises on the  
421 main ribs and the intercalary ribs become more frequent (stage *ii**b*, Fig. 4N1-  
422 N3). Rarely, the main ribs can be looped (Fig. 5Q1) or the intercalary ribs may  
423 be absent (Fig. 5C, D). Alternation between main and intercalary ribs is  
424 generally regular (Fig. 4K, O1-O3), but it can be irregular in some cases. In both  
425 stages *ii**a* and *ii**b*, the lateroventral tubercles are larger than the other tubercles.  
426 They are conical or claviform but their shape is altered by *post mortem*



427 deformation. Transition between stages *ii*a and *ii*b is very variable from a  
428 specimen to another. Stage *ii* ends between the beginning (Fig. 5O1) and the end  
429 of the flexus (Fig. 5F1, F2).

430 - Stage *iii* is in most of the cases composed of simple, dense, straight, flattened  
431 or sharp uniform ribs (rochi ribs, Fig. 7A, B1). They can be attenuated (Fig. 5E)  
432 or not (Fig. 5K1, K2) on the ventral area. They rarely bear a lateroventral  
433 tubercle (generally discrete, Fig. 5E), or lateral and lateroventral tubercles (Fig.  
434 5F1, F2). Some specimens exhibit rare royerianus ribs (Fig. 7C).

435 The dorsal area of the proversum, the flexus and the retroversum bear thin and  
436 dense ribs, concave toward the peristome (Fig. 4J2, N3, O3). No specimen has  
437 its peristome preserved. Septa can be observed on several specimens but the  
438 suture line is too poorly preserved to be studied. The phragmocone can occupy  
439 the whole proversum and the beginning of the flexus (Figs. 4P2, 5H1, O1, 7A,  
440 F). On several specimens, the last septum is located in the proversum (Figs. 4J1,  
441 L, N1, 5L).

442 The proportion of rochi ribs was calculated for 52 specimens, including 51  
443 specimens from GRS1 section. In this last section, the mean proportion of rochi  
444 ribs varies from 91.59% to 96.17% from Bed 99 to Bed 106, with a total mean  
445 value of 94.52% (Table 1). The histogram of rochi ribs proportion shows a

446 continuous, unimodal and strongly negatively skewed distribution (Fig. 8). It  
447 significantly departs from normality ( $p=0$ ).

448

449 *Description of the sample of the D. dufrenoyi Subzone.* Only 3 specimens were  
450 collected in the *D. dufrenoyi* Subzone. SBC06061/00001/GRS586 (GRS1, Bed  
451 110), figured in Bert and Bersac (2011, fig. 42) and SBC06061/00001/GRS728  
452 (GRS1, Bed 113) are fragments of proversum adorned with dense, straight,  
453 uniform and prorsiradiate ribs bearing a discrete lateroventral tubercle (stage *i*).  
454 SBC06061/00001/GRS731 (GRS1, Bed 113 figured Fig. 70) is a very poorly  
455 preserved fragment of proversum, flexus and retroversum. The proversum bears  
456 trituberculate ribs separated by one or two intercalaries. The ornamentation on  
457 the flexus and retroversum cannot be studied and the proportion of rochi ribs  
458 cannot be calculated.

459

460 *Variability and homogeneity of the Toxoceratoides of the D. furcata Zone of the*  
461 *LFAB.* As far as possible, ammonite populations have to be studied from a  
462 restricted stratigraphic interval in order to avoid time-averaging (see discussion  
463 in de Baets et al., 2015, p. 363). This is the case of our sample, which is  
464 restricted to the *D. furcata* Subzone, excepting 3 poorly preserved specimens

465 from the *D. dufrenoyi* Subzone. The following interpretations are thus based on  
466 the sample of the *D. furcata* Subzone only.

467 This sample has a very important morphological disparity. This variability is  
468 continuous and similar in every beds (Fig. 9). In GRS1 section, which provides  
469 most of the specimens of the *D. furcata* Subzone, changes from a bed to another  
470 are limited to a slight increase of H and a slight increase of the proportion of  
471 rochi ribs (Table 1). The value of H allows estimating adult size in tripartite  
472 ammonites (see discussion in Bersac and Bert 2020). Consequently, we consider  
473 a progressive increasing adult size of the *Toxoceratoides* through the *D. furcata*  
474 Subzone of the LFAB.

475 We interpret the morphological disparity of the sample of the *D. furcata* Zone as  
476 being driven by several processes (Fig. 9):

477 - The variation in duration of the ontogenetic stages: this corresponds to a  
478 process of heterochronic type that plays a significant role in ammonoid  
479 intraspecific variability in general (De Baets et al., 2015; Vennari and Aguirre-  
480 Urreta, 2019);

481 - The variation of the ornamentation of each ontogenetic stage: within each  
482 stage, there is a variation in rib density and in the number of intercalary ribs.  
483 This kind of ‘multipolar’ variability is extensively documented among  
484 ammonoids (Bert, 2013, De Baets et al., 2015). In stage *iii*, this variability

485 concerns in addition the proportion of rochi ribs. This proportion continuously  
486 varies from a specimen to another (Fig. 8). Its strongly negatively skewed  
487 distribution (which thus significantly departs from normality) can be due to the  
488 fact that the proportion of rochi ribs in this sample tends toward the value of  
489 100%, without, naturally, exceeding it.

490 - The delayed disappearance of a character through ontogeny: it could explain  
491 the presence of ribs with lateroventral and/or lateral tubercles (characteristic of  
492 the main ribs of stage *ii*) in some specimens' stage *iii*. Such phenomenon was  
493 described in the lower Aptian ammonite genus *Cheloniceras* Hyatt, 1903  
494 (Bersac and Bert, 2018);

495 - *H* varies in a continuous way by a factor 2 and its distribution does not  
496 significantly depart from normality (Fig. 6), which suggests a variation of the  
497 adult size in the same way. Such significant variation has already been  
498 documented among heteromorph tripartite ammonites (Landman, 1987; see  
499 discussion in Bersac and Bert, 2020);

500 - The variation of coiling (more or less curved proversum, variable angle  
501 between proversum and retroversum). This kind of variability among  
502 heteromorph ammonites has already been described (Kakabadze, 2004; Bert,  
503 2013; Delanoy et al., 2013; Bersac and Bert, 2020), especially in other  
504 representatives of the family Helicancyliidae (*Helicancyclus bonarellii* (Leanza,

505 1970) in Aguirre-Urreta, 1986, p. 292, fig. 13A-F; *Toxoceratoides nagerai*  
506 (Leanza, 1970) in Aguirre-Urreta, 1986, p. 298, fig. 16A-D, 17A-D).

507 The variability of the sample of the *D. furcata* Subzone appears to be continuous  
508 and involves processes already observed in other ammonite monospecific  
509 samples. Consequently, we interpret this sample as being monospecific. Such  
510 continuous variability is not involved by sexual dimorphism (see Bert, 2013,  
511 2019 for a description of the various rules of ammonoid intraspecific  
512 variability).

513 Although they are fragmentary, we have no argument to taxonomically isolate  
514 the three specimens of the *D. dufrenoyi* Subzone from the rest of the sample.

515

516 *Taxonomic attribution and consequences.* The sample of *Toxoceratoides* of the  
517 *D. furcata* Zone of the LFAB is characterized by the predominance of rochi ribs  
518 in its stage *iii*; its biostratigraphic position is also similar to that of *T. rochi* in its  
519 type locality (Frau et al., 2017, p. 340). For these reasons, we assigned this  
520 sample to *T. rochi*.

521 This interpretation implies that the disparity of *T. rochi* encompasses  
522 morphologies corresponding to several species of *Toxoceratoides*, but also  
523 morphologies that are atypical among *Toxoceratoides* and which are often

524 assigned to other genera of Helicancyllidae. Therefore, slender specimens with  
525 long stage *i* (i.e. with feebly tuberculate proversum, Fig. 7G) resemble the genus  
526 *Tonohamites*. Among the Helicancyllidae, co-occurrence of specimens with  
527 feebly tuberculate proversum and specimens with tuberculate proversum was  
528 already observed in the *D. grandis* Subzone of southern England by Casey  
529 (1960, 1961a). This author assigned the feebly tuberculate specimens to the  
530 genus *Tonohamites* and the tuberculate specimens to the genera *Tonohamites*  
531 and *Toxoceratoides*. Specimens with a stage *ii* essentially composed of main ribs  
532 (i.e. without intercalaries, Fig. 5D) mimic representatives of the genus  
533 *Helicancyllus* Gabb, 1869 or the species *Toxoceratoides krenkeli* Förster, 1975  
534 (Förster, 1975; Aguirre-Urreta, 1986). Fragments with such ornamentation from  
535 the *C. parinodum* Subzone (= *D. multicostatus* Subzone of Bersac et al., 2012)  
536 and the *D. grandis* Subzone of southern England were described under  
537 *Toxoceratoides* cf. *fustiformis* (von Koenen, 1902) by Casey (1961a, p. 83, pl.  
538 XVII, fig. 4). Large sized robust specimens resemble *Toxoceratoides stefanescui*  
539 Avram, 2002 (Avram, 2002, this species is regarded as a junior synonym of *T.*  
540 *rochi* by Frau et al., 2017). Specimens with slender stage *ii* (main ribs separated  
541 by several intercalaries, Figs. 5H, 7A) are similar to *Toxoceratoides transitorius*  
542 Avram, 2002. Small fragments of proversum bearing a stage *i* look like  
543 *Toxoceratoides emericianum* (d'Orbigny, 1842), etc.

544 *Biostratigraphic distribution. Dufrenoyia furcata* and *Dufrenoyia dufrenoyi*  
545 subzones (*Dufrenoyia furcata* Zone) and probably upper part of *Deshayesites*  
546 *grandis* Subzone (*Deshayesites deshayesi* Zone) of southern England.

547

548 3.2. Evolutionary patterns of the *Toxoceratoides* of the LFAB (Fig. 10)

549

550 The interpretations proposed in this chapter are based on data from the LFAB  
551 only. The proportion of rochi ribs in the *D. furcata* Zone could have been  
552 quantified in several beds only in GRS1 section (Table 1): we thus have studied  
553 the evolution of this character only in this section.

554

555 3.2.1. From the *D. forbesi* Zone to the *D. grandis* Subzone

556

557 In this interval, the *Toxoceratoides*:

558 - belong to the species *T. royerianus*;

559 - have a small population. In the *D. forbesi* Zone and the *D. multicosatus*  
560 Subzone, the population size of *Toxoceratoides* could have been small, as  
561 suggested by the very small number of specimens collected (2 specimens, see

562 Supplementary Appendix). In the *D. grandis* Subzone, the population size  
563 slightly increases (Bersac and Bert, 2019, fig. 18);

564 - have a low proportion of rochi ribs that may slowly increase over time (Table  
565 1);

566 - have a globally robust shape in the *D. grandis* Subzone (stage *ii* with strong  
567 tuberculate ribs separated by one atuberculate rib and stage *iii* bearing bifid and  
568 monotuberculate royerianus ribs). Note that in the earlier levels of the LFAB,  
569 the specimens are too fragmentary to determine their robustness.

570

571 3.2.2. From the *D. grandis* Subzone to the *D. furcata* Zone

572

573 - The population size of *Toxoceratoides* sharply increases (Bersac and Bert,  
574 2019, fig. 18).

575 - The proportion of rochi ribs sharply increases at the same time, rising from  
576 about 50% to 92% (Table 1).

577 - The specimens are more slender on average, due to a significant intraspecific  
578 variability.



579 These abrupt evolutionary changes compared to the precedent interval represent  
580 a speciation event that determines the transition from *T. royerianus* to *T. rochi*.  
581 This event could occur during the late *D. grandis* Subzone (see Chapter 3.1,  
582 ‘discussion’ of the systematic palaeontology of *T. royerianus*).

583 It is to note that we could not highlight in the LFAB the evolution of the  
584 lateroventral tubercles of stage *ii* described by Bulot et al. (2018), due to *post*  
585 *mortem* deformation of the specimens.

586

587 3.2.3. During the *D. furcata* Zone

588

589 - The proportion of *rochi* ribs continues to increase, but slower than before (from  
590 about 92% to 96%, see Table 1).

591 - The adult size of the specimens seems to slowly increase (see H in Table 1).

592

593 4. Conclusion

594

595 *T. sp.*, *T. royerianus* and *T. rochi* have been recognized within our sample of  
596 *Toxoceratoides* from the *D. forbesi* Zone - *D. furcata* Zone interval of the  
597 LFAB.

598 The large size of our sample of *Toxoceratoides rochi* (133 specimens) allowed  
599 highlighting the unprecedented range of morphological disparity of this species.  
600 This disparity is so significant that it encompasses the morphology of several  
601 species of *Toxoceratoides* and even of some genera of Helicancyliidae  
602 (*Tonohamites*, *Helicancyllus*). Nevertheless, additional data are necessary to  
603 decide if some of these taxa can be synonymized or not with *T. rochi* and  
604 *Toxoceratoides* respectively. If we had applied a typological concept of the  
605 species to the sample studied, we would probably have recognized dozens of  
606 species and several genera of Helicancyliidae.

607 Concerning the evolutionary patterns, the proportion of rochi ribs seems to be  
608 characterized by periods of slow increase separated by a sudden significant  
609 increase between the *D. grandis* Subzone and the *D. furcata* Subzone. This  
610 sudden increase, that occurs in a transgressive context (Bersac and Bert, 2019),  
611 is contemporaneous with the sharp increase ('bloom') of the population size of  
612 *Toxoceratoides*, which constitutes a speciation event determining the transition  
613 from *T. royerianus* to *T. rochi*. These elements suggest that the evolution of

614 *Toxoceratoides* could correspond to a punctuated equilibrium model (Eldredge  
615 and Gould, 1972) rather than a gradualist model.

616 The increasing trend in H highlighted in our samples is based on the study of  
617 frequently deformed specimens. As a consequence, this trend has to be  
618 confirmed by studying contemporaneous populations of non-deformed  
619 *Toxoceratoides* from other paleogeographic areas.

620 The proportion of rochi ribs in *Toxoceratoides* may be used as a complementary  
621 biostratigraphic tool. However, it would be necessary to study this parameter in  
622 larger samples from the *D. grandis* Subzone and from earlier biostratigraphic  
623 units to confirm this proposition. It would also be interesting to determine if this  
624 parameter could be modulated or not by paleogeography.

625

626 Disclosure of interest

627

628 The authors declare that they have no competing interest.

629

630 Acknowledgements

631

632 We warmly thank the Editor-in-Chief, the Associate Editor, Yves Dutour (Aix-  
633 en-Provence, France) and an anonymous reviewer. Their carefull reviewing and  
634 their relevant and valuable comments greatly helped to improve the manuscript.

635

636 References

637

638 Aguirre-Urreta, M. B., 1986. Aptian ammonites from the Argentinian Austral  
639 Basin, the subfamily Helicancylinae, Hyatt, 1894. Annals of the South African  
640 Museum 96 (7), 271-314.

641

642 Amédéo, F., Matrimon, B., 2004. Les ammonites aptiennes des Argiles à  
643 Plicatules de la bordure orientale du bassin de Paris: un aperçu. Bulletin de  
644 l'Association Géologique Audoise 24-25, 75-80.

645

646 Avram, E., 2002. Representatives in Romania of the genera *Dissimilites* Sarkar,  
647 1954 and *Toxoceratoides* Spath, 1924 (Ancyloceratina, Ammonoidea). Acta  
648 Palaeontologica Romaniaae 3 (2001), 23-30.

649

650 Baraboshkin, E.Y., Mikhailova, I.A., 2002. New stratigraphical scheme of the  
651 Lower Aptian of Middle Volga area. *Stratigraphy and Geological Correlation*  
652 10,  
653 82-105.

654

655 Bersac, S., Bert, D., Matrion, B, 2012. Revision of the index-species  
656 *Deshayesites deshayesi* (Ammonoidea, lower Aptian, Lower Cretaceous):  
657 Taxonomic and biostratigraphic consequences. In: Bersac, S. and Bert, D.  
658 (Eds.), First meeting of the Research Group for Paleobiology and  
659 Biostratigraphy of the Ammonites. *Boletin del Instituto de Fisiografia y*  
660 *Geologia* 82, 31-33.

661

662 Bersac, S., Bert, D., 2015. Two ammonite species under the same name:  
663 revision of *Deshayesites deshayesi* (d'Orbigny, 1841) based on toptype  
664 material (lower Aptian, Lower Cretaceous, Northeast of France). *Annales de*  
665 *Paléontologie* 101(4), 265-294.

666

667 Bersac, S., Bert, D., 2018. Revision of the lower Aptian (Lower Cretaceous)  
668 ammonite species *Chelonicerias cornuelianum* (d'Orbigny, 1841). *Annales de*  
669 *Paléontologie* 104(1), 45-70.

670

671 Bersac, S., Bert, D., 2019. The lower Aptian ammonites of the Les Ferres Aptian  
672 Basin (Lower Cretaceous, Southeast of France). Part I: Introduction and  
673 biostratigraphy. *Carnets de Géologie (Notebooks on Geology)* 19(9), 149-183.

674

675 Bersac, S., Bert, D., 2020. The heteromorph ammonite genus *Ancyloceras*  
676 (*Ancyloceratidae*) in the Paris Basin (lower Aptian, Lower Cretaceous,  
677 Northeast of France). *Annales de Paléontologie* 106 (2).  
678 <https://doi.org/10.1016/j.annpal.2019.102365>.

679

680 Bert, D., 2009. Description de *Artareites landii* nov. (Ammonoidea) du  
681 Barrémien supérieur de Majastre (Sud-Est de la France) et discussion sur les  
682 *Helicancyllidae* Hyatt, 1894. *Annales de Paléontologie* 95 (3), 139-163.

683

684 Bert, D., 2013. Factors of intraspecific variability in ammonites, the example of  
685 *Gassendiceras alpinum* (d'Orbigny, 1850) (Hemihoplitidae, Upper Barremian).  
686 *Annales de Paléontologie* 100 (3), 217-236.

687

688 Bert, D., 2019. Les lois de la variabilité intraspécifique chez les  
689 ammonites. Congrès de l'Association Paléontologique Française (APF), April  
690 2019, Aix-en-Provence, France.

691

692 Bert, D., Bersac, S., 2011. Buts et méthodes du "levé de coupe". *Fossiles* 6, 49-  
693 61.

694

695 Bulot, L.G., 2010. Appendix. Systematic paleontology of Aptian and Albian  
696 ammonites from southwest Iran. In: Vincent, B., van Buchem, F.S.P., Bulot,  
697 L.G., Immenhauser, A., Caron, M., Baghbani, D., Huc, A.Y. (Eds.), Carbon-  
698 isotope stratigraphy, biostratigraphy and organic matter distribution in the  
699 Aptian-Lower Albian successions of southwest Iran (Dariyan and Kazhdumi  
700 formations). *GeoArabia Special Publication* 4, 167-197.

701

702 Bulot, L. G., Frau, C., Pictet, A., 2018. Revision of *Toxoceratoides*  
703 *royeri* (d'Orbigny, 1842) and its bearing on the systematics of the Aptian  
704 Acrioceratidae Vermeulen, 2004 (Ammonoidea, Ancyloceratina,  
705 Ancyloceratoidea). *Cretaceous Research* 88, 187-196.

706

707 Casey, R., 1960. A monograph of the Ammonoidea of the Lower Greensand,  
708 part I. *Palaeontographical Society* (1959), i-xxxxvi + 1-44.

709

710 Casey, R., 1961a. A monograph of the Ammonoidea of the Lower Greensand,  
711 part II. *Palaeontographical Society* (1960), 41-118.

712

713 Casey, R., 1961b, The stratigraphical palaeontology of the Lower Greensand.  
714 *Palaeontology*, London. Volume 3, 487-621.

715

716 Casey, R., 1980. A monograph of the Ammonoidea of the Lower Greensand, part  
717 IX. *Palaeontographical Society*, London, 633-660.

718

719 Casey, R., Bayliss, H.M., Simpson, M.I., 1998. Observations on the  
720 lithostratigraphy and ammonite succession of the Aptian (Lower Cretaceous)



721 Lower Greensand of Chale Bay, Isle of Wight, UK. *Cretaceous Research* 19,  
722 511-535.

723

724 Conte, G., 1999. Éléments de la faune de l'Aptien inférieur (Bédoulien) de  
725 Serviers-La-Baume (Gard). *Bulletin de la Société d'Etude des Sciences*  
726 *Naturelles de Nîmes et du Gard* 62, 11-15.

727

728 Corroy, G., 1925. *Le Néocomien de la bordure orientale du Bassin de Paris.*  
729 Imprimerie J. Coubé and Fils, Nancy.

730

731 De Baets, K., Bert, D., Hoffmann, R., Monnet, C., Yacobucci, M.M., Klug, C.,  
732 2015. Ammonoid intraspecific variability. In: Klug, C., Korn, D., De Baets, K.,  
733 Kruta, I., Mapes, R.H. (Eds.), *Ammonoid paleobiology: from anatomy to*  
734 *ecology. Topics in Geobiology* 43, 359-426.

735

736 Delanoy, G., Baudouin, C., Gonnet, R., Bert, D., 2008. Sur les faunes  
737 d'ammonites (Crétacé inférieur) du niveau glauconieux de la carrière des Trois-  
738 Vernes, près de Crest (Drôme, Sud-est de la France). *Annales du Muséum*  
739 *d'Histoire Naturelle de Nice* XXIII, 11-65.

740

741 Delanoy, G., Moreno-Bedmar, J. A., Ruiz, J. J., Tolós Llàdser, D., 2013.  
742 *Xerticeras* gen. nov., a new genus of micromorphic heteromorph ammonite  
743 (Ancyloceratina, Ancyloceratidae) from the lower Aptian of Spain. Carnets de  
744 Géologie [Notebooks on Geology], Brest, Article 2013/02 (CG2013\_A02), 89-  
745 103.

746

747 Eldredge, N., Gould, S.J., 1972. Punctuated equilibria: An alternative to phyletic  
748 gradualism. In: Schopf, T. J. M. (Ed.), Models in Paleobiology. Freeman-  
749 Cooper & Co., San Francisco, 82-115.

750

751 Förster, R., 1975. Die geologische Entwicklung von Süd-Mozambique seit der  
752 Unterkreide und die Ammoniten-Fauna von Unterkreide und Cenoman.  
753 Geologisches Jahrbuch (B) 12, 3-324.

754

755 Frau, C., Bulot, L.G., Delanoy, G., 2017. New and poorly known Aptian  
756 Acrioceratidae (Ancyloceratoidea, Ammonoidea) from Cassis - Roquefort-la-  
757 Bédoule (Bouches-du-Rhône). Neues Jahrbuch für Geologie und Paläontologie  
758 Abhandlungen 238 (3), 335-346.

759

760 Hammer, O., Harper, D.A.T., 2006. Paleontological data analysis. Blackwell  
761 publishing, Oxford.

762

763 Hammer, O., Harper, D.A.T., Ryan, P.D., 2001. PAST: Paleontological  
764 Statistics Software Package for Education and Data Analysis. *Palaeontologia*  
765 *Electronica* 4 (1), 9 p.

766

767 Kakabadze M. V., 2004. Intraspecific and intrageneric variabilities and their  
768 implication for the systematics of Cretaceous heteromorph ammonites; a review.  
769 *Scripta Geologica* 128, 17-37.

770

771 Kakabadze, M. V., Hoedemaeker, P. J., 2004. Heteromorphic ammonites from  
772 the Barremian and Aptian strata of Colombia. *Scripta Geologica* 128, 39-182.

773

774 Klein, J., Busnardo, R., Company, M., Delanoy, G., Kakabadze, M., Reboulet,  
775 S., Ropolo, P., Vašíček, Z., Vermeulen, J., 2007. *Fossilium Catalogus I:*  
776 *Animalia. Pars 144. Lower Cretaceous Ammonites III. Bochianitoidea,*  
777 *Protancyloceratoidea, Ancyloceratoidea, Ptychoceratoidea. Backhuys*  
778 *Publishers, Leiden.*

779

780 Landman, N.H., 1987. Ontogeny of Upper Cretaceous (Turonian-Santonian)  
781 scaphitid ammonites from the Western Interior of North America: systematics,  
782 developmental patterns, and life history. *Bulletin of the American Museum of*  
783 *Natural History* 185 (2), 117-241.

784

785 Mikhailova, I.A., Baraboshkin, E.J., 2002. *Volgoceratoides* and *Koeneniceras* -  
786 new small-size Lower Aptian heteromorphs from the Ulijanovsk Region  
787 (Russian Platform). *Abhandlungen der Geologischen Bundesanstalt* 57, 539-  
788 553.

789

790 Reboulet, S., Szives, O., Aguirre-Urreta, B., Barragan, R., Company, M.,  
791 Idakieva, V., Ivanov, M., Kakabadze, M.V., Moreno-Bedmar, J.A., Sandoval, J.,  
792 Baraboshkin, E.J., Caglar, M.K., Fozy, I., González-Arreola, C., Kenjo, S.,  
793 Lukeneder, A., Raisossadat, S.N., Rawson, P.F., Tavera, J.M., 2014. Report on  
794 the 5th International Meeting of the IUGS Lower Cretaceous Ammonite  
795 Working Group, the “Kilian Group” (Ankara, Turkey, 31st August 2013).  
796 *Cretaceous Research* 50, 126-137.

797

798 Reboulet, S., Szives, O., Aguirre-Urreta, B., Barragan, R., Company, M., Frau,  
799 C., Kakabadze, M.V., Klein, J., Moreno-Bedmar, J.A., Lukeneder, A., Pictet, A.,

800 Ploch, I., Raisossadat, S.N., Vašíček, Z., Baraboshkin, E.J., Mitta, V.V., 2018.  
801 Report on the 6<sup>th</sup> International Meeting of the IUGS Lower Cretaceous  
802 Ammonite Working Group, the “Kilian Group” (Vienna, Austria, 20<sup>th</sup> August  
803 2017). *Cretaceous Research* 91, 100-110.

804

805 Vennari, V.V., Aguirre-Urreta, M.B., 2019. Intraspecific variability,  
806 biostratigraphy and paleobiological significance of the Southern Gondwana  
807 ammonoid genus *Lytohoplites* Spath. *Journal of Paleontology* 93 (4), 702-726.

808

809 Vermeulen, J., 2004. Vers une nouvelle classification à fondement  
810 phylogénétique des ammonites hétéromorphes du Crétacé inférieur  
811 méditerranéen. Le cas des Crioceratitidae Gill, 1871, nom. correct., 1952, des  
812 Emericiceratidae fam. nov. et des Acrioceratidae fam. nov. (Ancylocerataceae  
813 Gill, 1871). *Riviera Scientifique*, 88, 69-92.

814

815 Figures, table and plates

816

817 Fig. 1. Map of the Les Ferres area with location of the sections that provided the  
818 studied material. Geographic coordinates of the sections: GRS1 (lat.:  
819 43.842177°, long.: 7.076508°), VAL (lat.: 43.842256°, long.: 7.09677°), GRO

820 (lat: 43.843379°, long: 7.1°), CHP (lat.: 43.845193°, long.: 7.102648°), CLE  
821 (lat.: 43.845193°, long.: 7.102648°). See online version for colours.

822

823 Fig. 2. Bio-chronostratigraphic charts used in the present work. SZS: Standard  
824 Mediterranean Zonal Scheme. St.: stages.

825

826 Fig. 3. *Toxoceratoides* shell morphological terminology and measured  
827 parameter. H: whorl height at the middle of the flexus.

828

829 Fig. 4. The arrow indicates the beginning of the body chamber. All specimens:  
830 Bersac's collection. A: *Toxoceratoides* sp., SBC.06061-00007/CLE036, CLE  
831 section, Bed 400, *Deshayesites forbesi* Zone. B: *Toxoceratoides royerianus*  
832 (d'Orbigny, 1842), SBC.06061-00003/VAL066, VAL section, Bed 405,  
833 *Deshayesites multicostatus* Subzone (*Deshayesites deshayesi* Zone). C-G:  
834 *Toxoceratoides royerianus* (d'Orbigny, 1842), *Deshayesites grandis* Subzone  
835 (*Deshayesites deshayesi* Zone). C: SBC.06061-00006/CHP359, CHP section,  
836 Bed 416. D: SBC.06061-00006/CHP041, CHP section, Bed 416. E: SBC.06061-  
837 00006/CHP038, CHP section, Bed 416. F: SBC.06061-00007/CLE004, CLE  
838 section, Bed 416. G: SBC.06061-00001/GRS510, GRS1 section, Bed 97. H-P:

839 *Toxoceratoides rochi* Casey, 1961, *Dufrenoyia furcata* Subzone (*Dufrenoyia*  
840 *furcata* Zone). H: SBC.06061-00001/GRS284, GRS1 section, Bed 102. I:  
841 SBC.06061-00001/GRS222, GRS1 section, Bed 102. J: SBC.06061-  
842 00001/GRS358, GRS1 section, Bed 100. K: SBC.06061-00005/GRO076, GRO  
843 section, Bed 418. L: SBC.06061-00001/GRS287, GRS1 section, Bed 102. M:  
844 SBC.06061-00001/GRS159, GRS1 section, Bed 100. N: SBC.06061-  
845 00001/GRS414, GRS1 section, Bed 104. O: SBC.06061-00001/GRS186, GRS1  
846 section, Bed 100. P: SBC.06061-00001/GRS398, GRS1 section, Bed 104.

847

848 Fig. 5: *Toxoceratoides rochi* Casey, 1961, GRS1 section, *Dufrenoyia furcata*  
849 Subzone (*Dufrenoyia furcata* Zone), Bersac's collection. The arrow indicates  
850 the beginning of the body chamber. A: SBC.06061-00001/GRS206, Bed 102. B:  
851 SBC.06061-00001/GRS238, Bed 102. C: SBC.06061-00001/GRS585, Bed 102.  
852 D: SBC.06061-00001/GRS527, Bed 104. E: SBC.06061-00001/GRS607, Bed  
853 102. F: SBC.06061-00001/GRS367, Bed 99. G: SBC.06061-00001/GRS366,  
854 Bed 99. H: SBC.06061-00001/GRS221, Bed 102. I: SBC.06061-  
855 00001/GRS591, Bed 102. J: SBC.06061-00001/GRS383, Bed 102. K:  
856 SBC.06061-00001/GRS579, Bed 102. L: SBC.06061-00001/GRS524, Bed 104.  
857 M: SBC.06061-00001/GRS289, Bed 102. N: SBC.06061-00001/GRS321, Bed

858 99. O: SBC.06061-00001/GRS580, Bed 102. P: SBC.06061-00001/GRS034,  
859 Bed 102. Q: SBC.06061-00001/GRS198, Bed 100.

860

861 Fig 6. Histogram of H (whorl height at the middle of the flexus in mm) of 57  
862 specimens of *Toxoceratoides rochi* Casey, 1961 from the *Dufrenoyia furcata*  
863 Subzone (*Dufrenoyia furcata* Zone, lower Aptian) of the Les Ferres Aptian  
864 Basin and result of the Shapiro-Wilk normality test. Black curve: fitted normal  
865 curve. Dark red curve: kernel density estimator. See online version for colours.

866

867 Fig. 7. The arrow indicates the beginning of the body chamber. All specimens:  
868 Bersac's collection. A-N: *Toxoceratoides rochi* Casey, 1961, *Dufrenoyia furcata*  
869 Subzone (*Dufrenoyia furcata* Zone). A: SBC.06061-00001/GRS224, GRS1  
870 section, Bed 102. B: SBC.06061-00001/GRS644, GRS1 section, Bed 102. C:  
871 SBC.06061-00001/GRS649, GRS1 section, Bed 106. D: SBC.06061-  
872 00001/GRS582, GRS1 section, Bed 102. E: SBC.06061-00006/CHP201, CHP  
873 section, Bed 421. F: SBC.06061-00001/GRS022, GRS1 section, Bed 102. G:  
874 SBC.06061-00001/GRS616, GRS1 section, Bed 99. H: SBC.06061-  
875 00001/GRS323, GRS1 section, Bed 99. I: SBC.06061-00001/GRS182, GRS1  
876 section, Bed 100. J: SBC.06061-00001/GRS046, GRS1 section, Bed 102. K:  
877 SBC.06061-00001/GRS522, GRS1 section, Bed 104. L: SBC.06061-



878 00001/GRS717, GRS1 section, Bed 102. M: SBC.06061-00001/GRS523, GRS1  
879 section, Bed 104. N: SBC.06061-00001/GRS127, GRS1 section, Bed 102. O:  
880 *Toxoceratoides rochi* Casey, 1961, SBC.06061-00001/GRS731, GRS1 section,  
881 Bed 113. *Dufrenoyia dufrenoyi* Subzone (*Dufrenoyia furcata* Zone).

882

883 Fig 8. Histogram of rochi ribs proportion of 52 specimens of *Toxoceratoides*  
884 *rochi* Casey, 1961 from the *Dufrenoyia furcata* Subzone (*Dufrenoyia furcata*  
885 Zone, lower Aptian) of the Les Ferres Aptian Basin section and result of the  
886 Shapiro-Wilk normality test.. Black curve: fitted normal curve. Dark red curve:  
887 kernel density estimator. See online version for colours.

888

889 Fig. 9. Patterns of intraspecific variability of *Toxoceratoides rochi* Casey, 1961.  
890 A: slightly curved proversum, intermediate angle between proversum and  
891 retroversum. B: substraight proversum, open angle. C: substraight proversum,  
892 narrow angle. D: stage *ii* with rare intercalary ribs, stage *iii* with rare royerianus  
893 ribs. E: stage *ii* with one intercalary rib between main ones on a regular basis,  
894 stage *iii* with only rochi ribs. F: stage *ii* with several intercalated ribs between  
895 primary ones, stage *iii* with rare royerianus ribs. G: early onset of stage *ii*, late  
896 onset of stage *iii*. H: later onset of stage *ii*, early onset of stage *iii*. I: very late  
897 ending of stage *i*, no stage *ii*. J: large size. K: intermediate size. L: small size.

898

899 Fig. 10. Evolutionary patterns of the genus *Toxoceratoides* Spath, 1924  
 900 according to Bulot et al. (2018) and this work. Biostratigraphic chart: see Fig. 2.

901

		Proportion of rochi ribs	H (mm)	
<i>Toxoceratoides rochi</i>	GRS 1 section (les Graous Member, <i>Dufrenoyia furcata</i> Subzone)	Bed 106	94.11 % (N=1)	18.8 (N=1)
		Bed 104	94.7 % (N=5)	13.88 (N=5)
		Bed 102	96.17 % (N=28)	13.47 (N=32)
		Bed 100	91.91 % (N=9)	12.95 (N=10)
		Bed 99	91.59 % (N=8)	11.97 (N=9)
<i>Toxoceratoides royerianus</i>	<i>Toxoceratoides</i> Bed ( <i>Deshayesites grandis</i> Subzone)	47.88 % (N=4)	10.04 (N=5)	
	<i>Ammonitoceras</i> Level ? ( <i>Deshayesites multicostratus</i> Subzone)	42.85 % (N=1)	13.9 (N=1)	
<i>Toxoceratoides</i> sp.	Top of HAL ( <i>Deshayesites forbesi</i> Zone)	0 % (N=1)	9 (N=1)	

902

903 Table 1. Mean values of the proportion of rochi ribs and whorl height at the  
904 middle of the flexus (H) of the taxa recognized in the present article. N =  
905 number of studied specimens. HAL = Hauterivian-Aptian limestones. Litho- and  
906 biostratigraphic charts after Bersac and Bert (2019) and Fig. 2.

Journal Pre-proof

**Declaration of interests**

The authors declare that they have no known competing financial interests or personal relationships that could have appeared to influence the work reported in this paper.

05<sup>th</sup> October 2020

Stéphane Bersac

Didier Bert

Journal Pre-proof